CHAPTER 5:

PVA DOPED WITH $Li_4Ti_5O_{12}$

CHAPTER 5

PVA DOPED WITH $Li_4Ti_5O_{12}$

5.1 Introduction

Standing films of PVA doped with different concentrations of $Li_4Ti_5O_{12}$ have been successfully prepared via the solution cast-technique. PVA was selected as the host due to its excellent film-forming capability [Mohan *et al*., 2010]. Shown in Figure 5.1 is the composite film of 92 wt. % PVA and 8 wt. % of $Li_4Ti_5O_{12}$. At low $Li_4Ti_5O_{12}$ concentration, the films were transparent but transformed to opaque upon addition of 10 wt. % of $Li_4Ti_5O_{12}$.

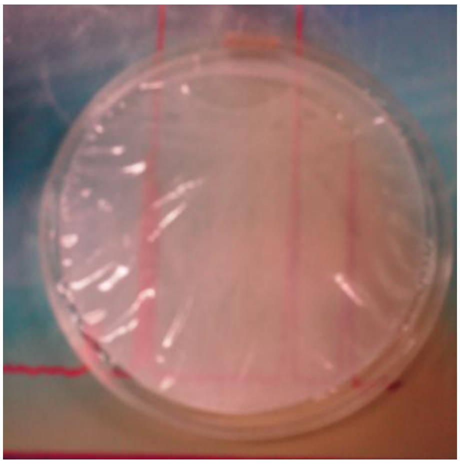

Figure 5.1: PVA film doped with 8 wt. % $Li_4Ti_5O_{12}$.

PVA-$Li_4Ti_5O_{12}$ composite films were characterized using x-ray diffraction (XRD), fourier transform infrared (FTIR) spectroscopy, Uv-vis spectroscopy, scanning electron microscopy (SEM) and electrochemical impedance spectroscopy (EIS) to determine physical and electrical properties.

5.2 X-ray diffraction (XRD)

Figure 5.2 shows the x-ray diffractogram of $Li_4Ti_5O_{12}$, PVA and PVA doped with different concentrations of $Li_4Ti_5O_{12}$. XRD profile of $Li_4Ti_5O_{12}$ shows peaks exhibited at $2\theta=18.55^o$, 35.90^o, 43.60^o, 47.85^o, 57.80^o, 63.40^o and 67.00^o. All the peaks have been reported by Raja et al., (2009). The peak at $2\theta=20.50^o$ is a Li_2TiO_3 peak and can be seen in Figure 5.2(a) [Wang *et al.*, 1999]. PVA films show two peaks at $2\theta=19.00^o$ and ~23.00^o.

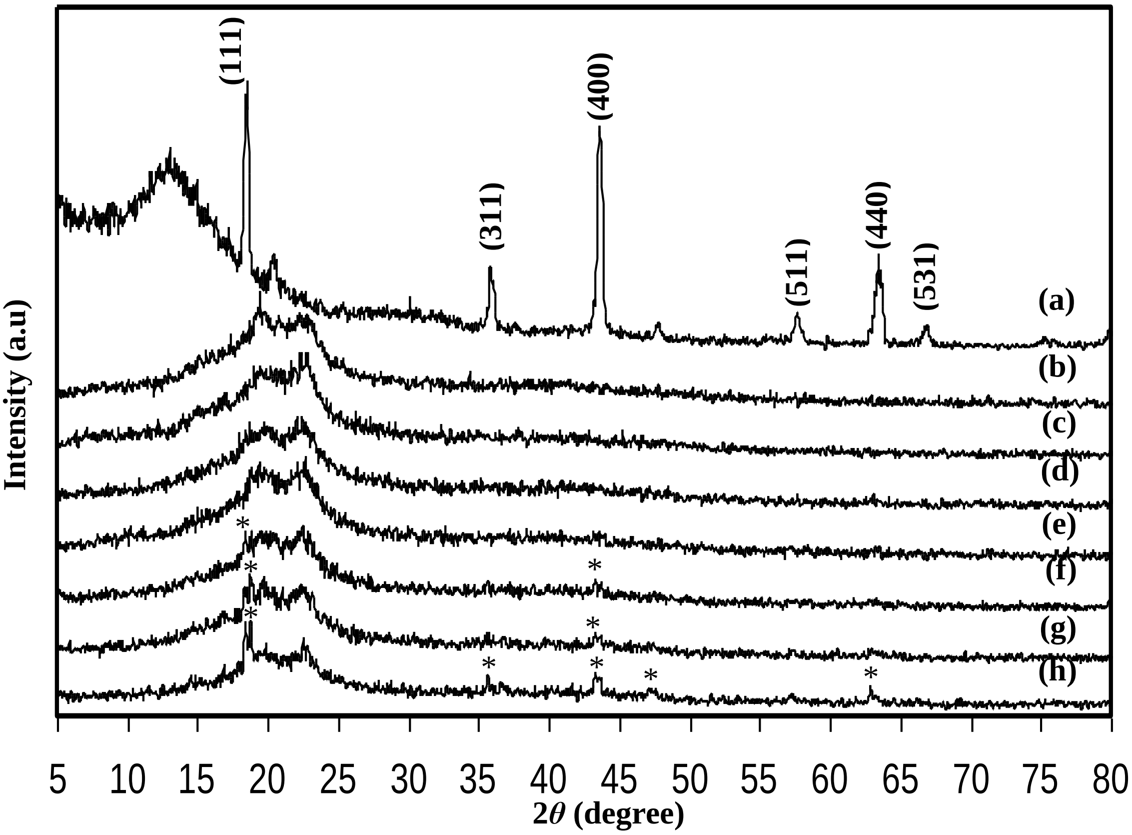

Figure 5.2: XRD profile of (a) $Li_4Ti_5O_{12}$, (b) film of PVA dissolved in water, (c) film of PVA dissolved in 1 % acetic acid and doped with (d) 2 wt. % $Li_4Ti_5O_{12}$, (e) 4 wt. % $Li_4Ti_5O_{12}$, (f) 6 wt. % $Li_4Ti_5O_{12}$, (g) 8 wt. % $Li_4Ti_5O_{12}$ and (h) 10 wt. % $Li_4Ti_5O_{12}$. (*) indicates $Li_4Ti_5O_{12}$.

Tawansi *et al.*, (2005) noted that PVA has a clear crystalline peak at scattering angle $2\theta=19.50^o$ which corresponds to a (101) spacing. The peak at $2\theta=22.90^o$ also implies the semi-crystallinity nature of PVA polymer and is assigned to (200) reflection

[Gautam and Ram, 2010]. With increase in addition of $Li_4Ti_5O_{12}$ into the PVA polymer peaks corresponding to $Li_4Ti_5O_{12}$ are exhibited in the XRD pattern of Figure 5.2 (e), (f), (g) and (h).

5.3 Fourier transform infrared (FTIR)

Tabulated in Table 5.1 are infrared peaks that can be ascribed to poly (vinyl alcohol) (PVA).

Table 5.1: Infrared peak assignments of PVA polymer.

Wavenumber (cm^{-1})	Assignments	References
850	C-C stretching	Tawansi *et al.*, (2005)
950	CH_2 stretching	Tawansi *et al.*, (2005)
1055, 1094, 1125 1122	C-O stretching	Lee *et al.*, (2008) Abdelaziz and Ghannam, (2010)
1140	C-O stretching (crystalline form)	Lee *et al.*, (2008)
1230	CH deformation	Lee *et al.*, (2008)
1331 1375 1320	CH_2 deformation	Lee *et al.*, (2008) Tawansi *et al.*, (2005)
1427 1424	CH_2 scissoring	Lee *et al.*, (2008) Tawansi *et al.*, (2005)
1653 1680 1571	C=C stretching	Lee *et al.*, (2008) Tawansi *et al.*, (2005) Abdelaziz and Ghannam, (2010)
1662	v(C=O)	Abdelaziz and Ghannam, (2010)
2940	$v_a\,(CH_2)$	Tawansi *et al.*, (1998)
3270	OH strecthing	Yang *et al.*, (2009)
3040	$RCH=CH_2$	Tawansi *et al.*, (1998)

Shown in Figure 5.3 (a) is the FTIR spectrum for the film of PVA dissolved in the water. The vibrational spectrum of PVA is related to the stretching and bending vibrations of O-H, C-O, C=O, C=C and C-H groups (Abdelaziz and Ghannam, 2010). The peak at 3173 cm^{-1} is due to the O-H stretching. The peak at 1740 cm^{-1} is attributed to the residual acetate groups (C=O) remaining after the manufacture of PVA from the hydrolysis of poly (vinyl acetate) or oxidation during manufacturing and processing [Yang *et al.*, 2009; Tawansi *et al.*, 1998]. Tawansi *et al.*, (1998; 2005) noted that the presence of double bond segments are considered as suitable sites for polarons or bipolarons. Figure 5.3(b) depicts the FTIR spectrum for PVA dissolved in 1 % acetic acid.

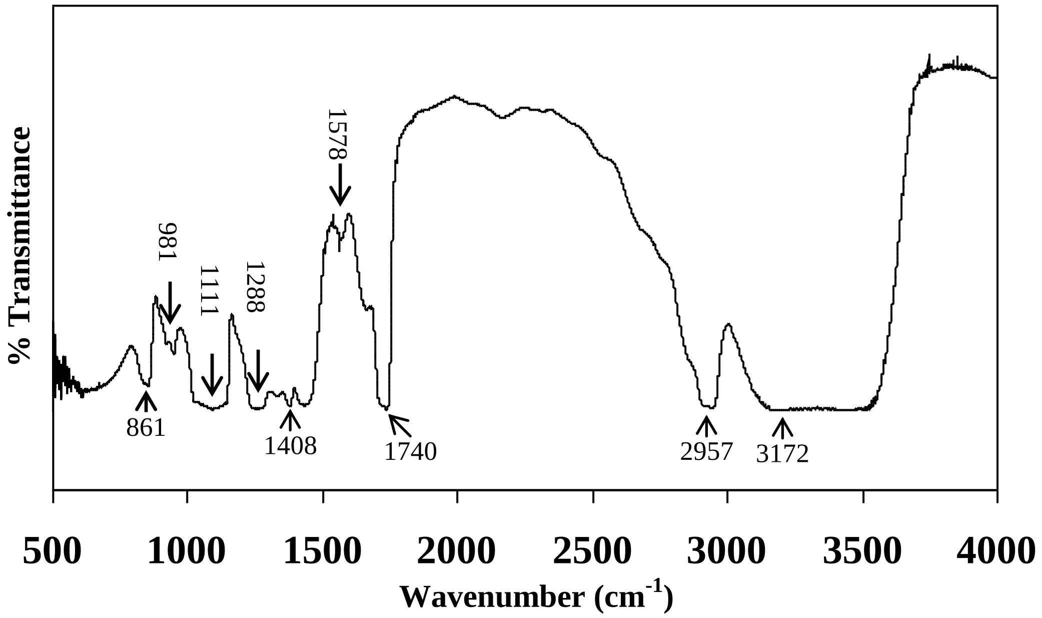

Figure 5.3(a): FTIR spectrum for film of PVA dissolve in water from 500 cm^{-1} to 4000 cm^{-1}.

Abdelaziz and Ghannam (2010) assigned the peak at 1571 cm^{-1} to C=C stretching of PVA polymer. It can be observed that the C=C stretching band for the film of PVA dissolved in water in this work is located at 1578 cm^{-1}. On the other hand, the peak corresponding to C=C stretching for the film of PVA dissolved in acetic acid is located at 1571 cm^{-1}. In the present work, the peak due to C=O stretching band for film for PVA dissolved in water is detected at 1740 cm^{-1}, Figure (5.3(a)). The C=O band for the PVA film in which 1 % acetic acid was used is located at 1745 cm^{-1}, Figure (5.3(b)).

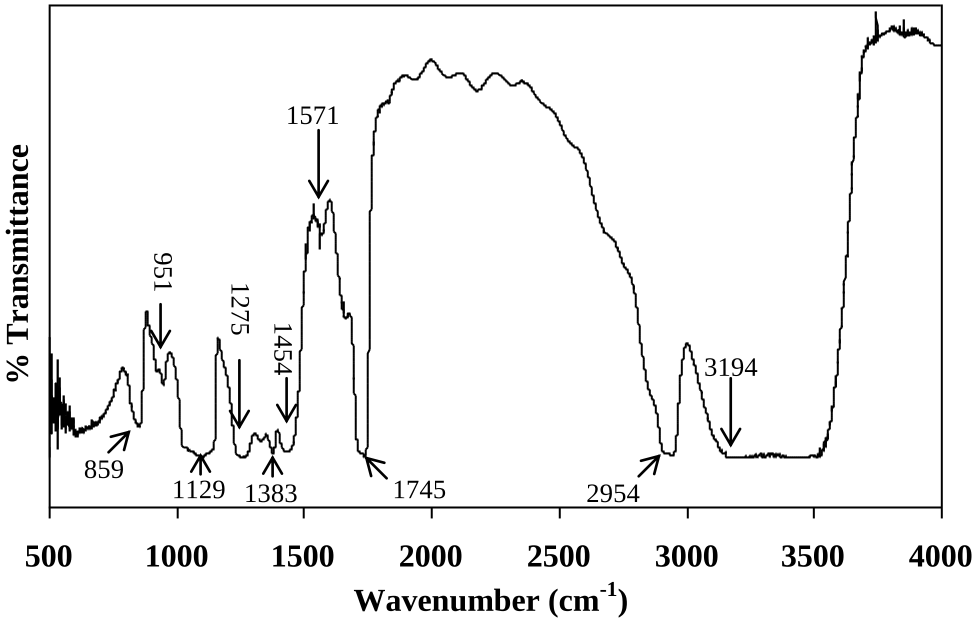

Figure 5.3(b): FTIR spectrum for film of PVA dissolved in 1 % of acetic acid from 500 cm^{-1} to 4000 cm^{-1}.

Shown in Figure 5.4 are the FTIR spectra of PVA dissolved in 1% acetic acid and doped with different amounts of $Li_4Ti_5O_{12}$ in the range between 1000 and 2000 cm^{-1}. After the addition of 2, 4, 6, 8 and 10 wt. % of $Li_4Ti_5O_{12}$, the C=C stretching band can be located at 1578 cm^{-1}, 1579 cm^{-1}, 1579 cm^{-1}, 1577 cm^{-1} and 1583 cm^{-1} respectively. In the context of the present investigation, these changes in wavenumber is due to weak interaction between $Li_4Ti_5O_{12}$ and the dipole induced during C=C stretching. Hence, the shifts in C=C wavenumber may also be considered as proof of occurrence of complexation.

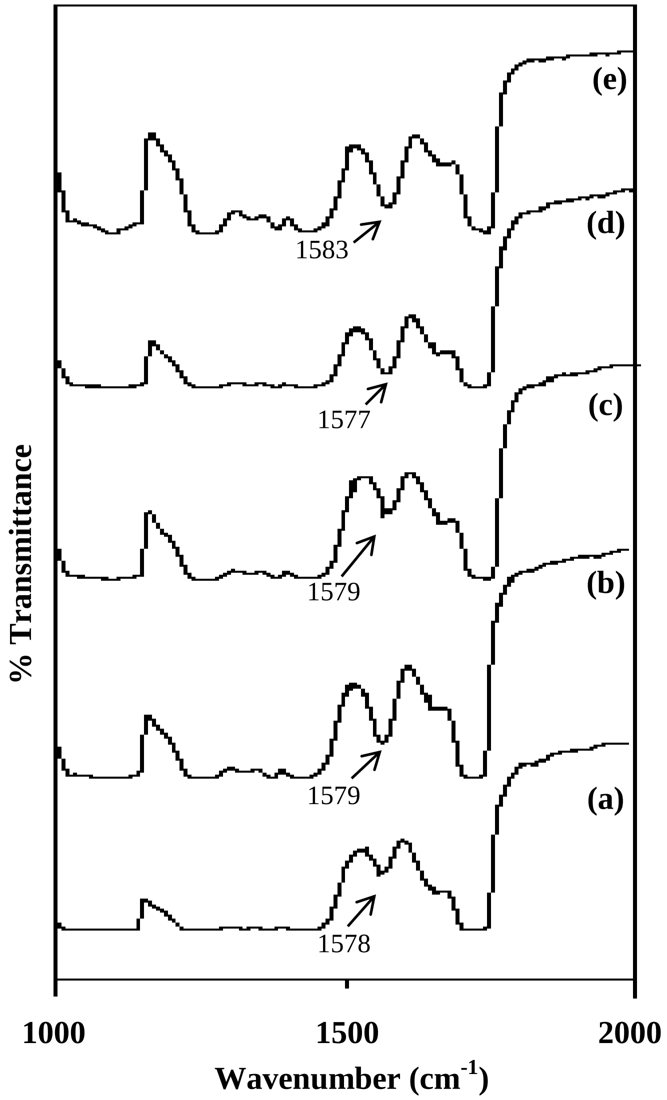

Figure 5.4: FTIR spectra of PVA film (dissolved in 1 % acetic acid) and doped with (a) 2 wt. % $Li_4Ti_5O_{12}$, (b) 4 wt. % $Li_4Ti_5O_{12}$, (c) 6 wt. % $Li_4Ti_5O_{12}$, (d) 8 wt. % $Li_4Ti_5O_{12}$ and (e) 10 wt. % $Li_4Ti_5O_{12}$.

Depicted in Figure 5.5 is FTIR spectra of film produced by dissolving PVA in 1 % acetic acid and doped with (a) 2 wt. % $Li_4Ti_5O_{12}$, (b) 4 wt. % $Li_4Ti_5O_{12}$, (c) 6 wt. % $Li_4Ti_5O_{12}$, (d) 8 wt. % $Li_4Ti_5O_{12}$ and (e) 10 wt. % $Li_4Ti_5O_{12}$. The bands due to CH_2 and OH stretching shifted from 2954 cm^{-1} and 3194 cm^{-1} (Figure 5.3(a)) to approximately 2940 and 3150 cm^{-1} for all PVA doped with different amounts of $Li_4Ti_5O_{12}$.

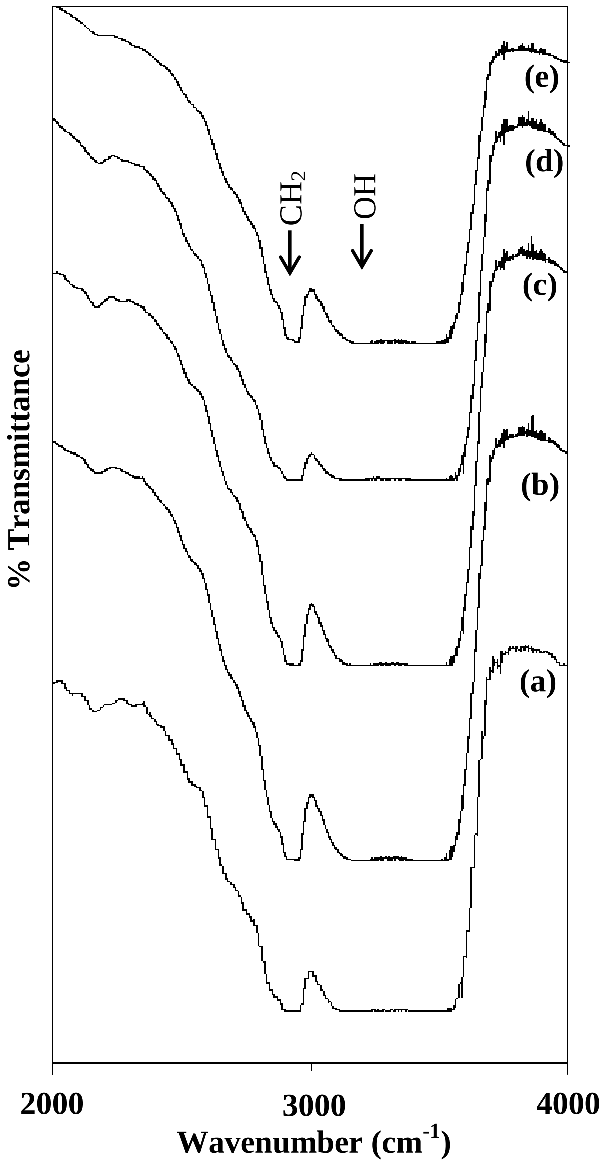

Figure 5.5: FTIR spectra of PVA film (dissolved in 1 % acetic acid) and doped with (a) 2 wt. % $Li_4Ti_5O_{12}$, (b) 4 wt. % $Li_4Ti_5O_{12}$, (c) 6 wt. % $Li_4Ti_5O_{12}$, (d) 8 wt. % $Li_4Ti_5O_{12}$ and (e) 10 wt. % $Li_4Ti_5O_{12}$ from 2000 cm^{-1} to 4000 cm^{-1}.

5.4 UV-Vis spectroscopy

The UV-Vis absorption spectrum for film dissolved in water and acetic acid are shown in Figure 5.6 (a) and (b) in the range from 200 nm to 900 nm. The PVA film obtained from casting the solution of the polymer in water and acetic acid exhibits an absorption edge (AE) at ~ 272.0 nm and 272.5 nm respectively. This indicates the semi-crystalline nature of PVA as reported by Abdelaziz and Ghannam, (2010) where the absorption edge (AE) has been reported at approximately 250 nm.

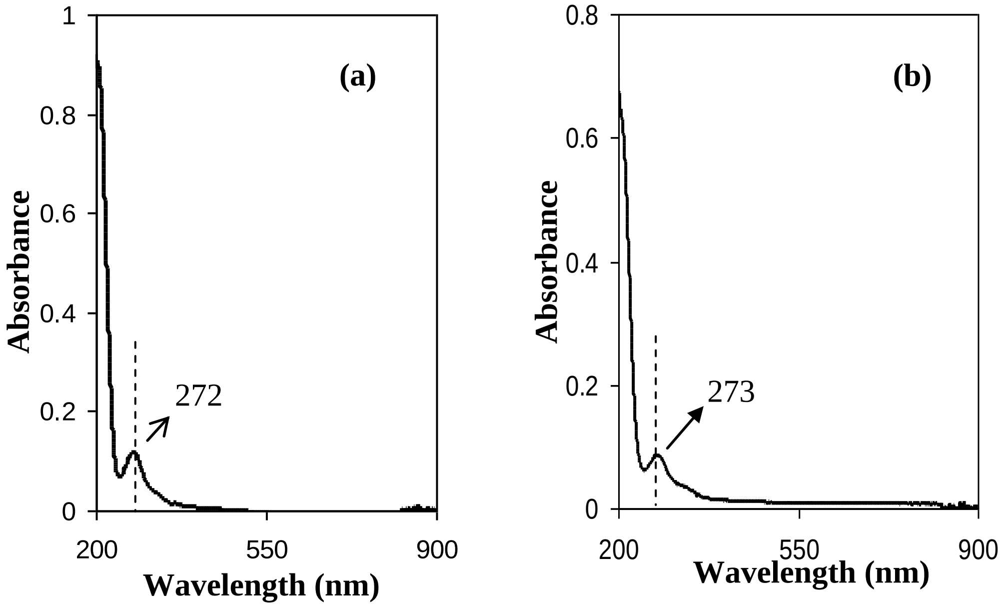

Figure 5.6: The UV-Vis absorption spectra of pure PVA film obtained from casting the solution of the polymer in (a) water and (b) acetic acid.

Shown in Figure 5.7 is UV-Vis spectra of PVA dissolved in 1 % acetic acid and doped with the various amount of $Li_4Ti_5O_{12}$ from 200 nm to 900 nm. After addition of 2 wt. % and 4 wt. % $Li_4Ti_5O_{12}$ the absorption edge due to the semi-crystalline PVA disappears. On addition of $Li_4Ti_5O_{12}$ from 6 wt. %, to 10 wt. %, the absorption edge is observed at 262 nm, 266 nm and 254 nm. This is attributed to intramolecular and intermolecular reaction between hydrogen and titanium ions [Abdelaziz and Ghannam, 2010]. Zidan (1999) reported that the absorption edge (AE) at 265 nm is due to the absorption by simple carbonyl group along the polymer chain. Likewise the absorption edge (AE) at 334 nm is assigned to $–C\text{-}(CH{=}CH)_3CO\text{-}$.

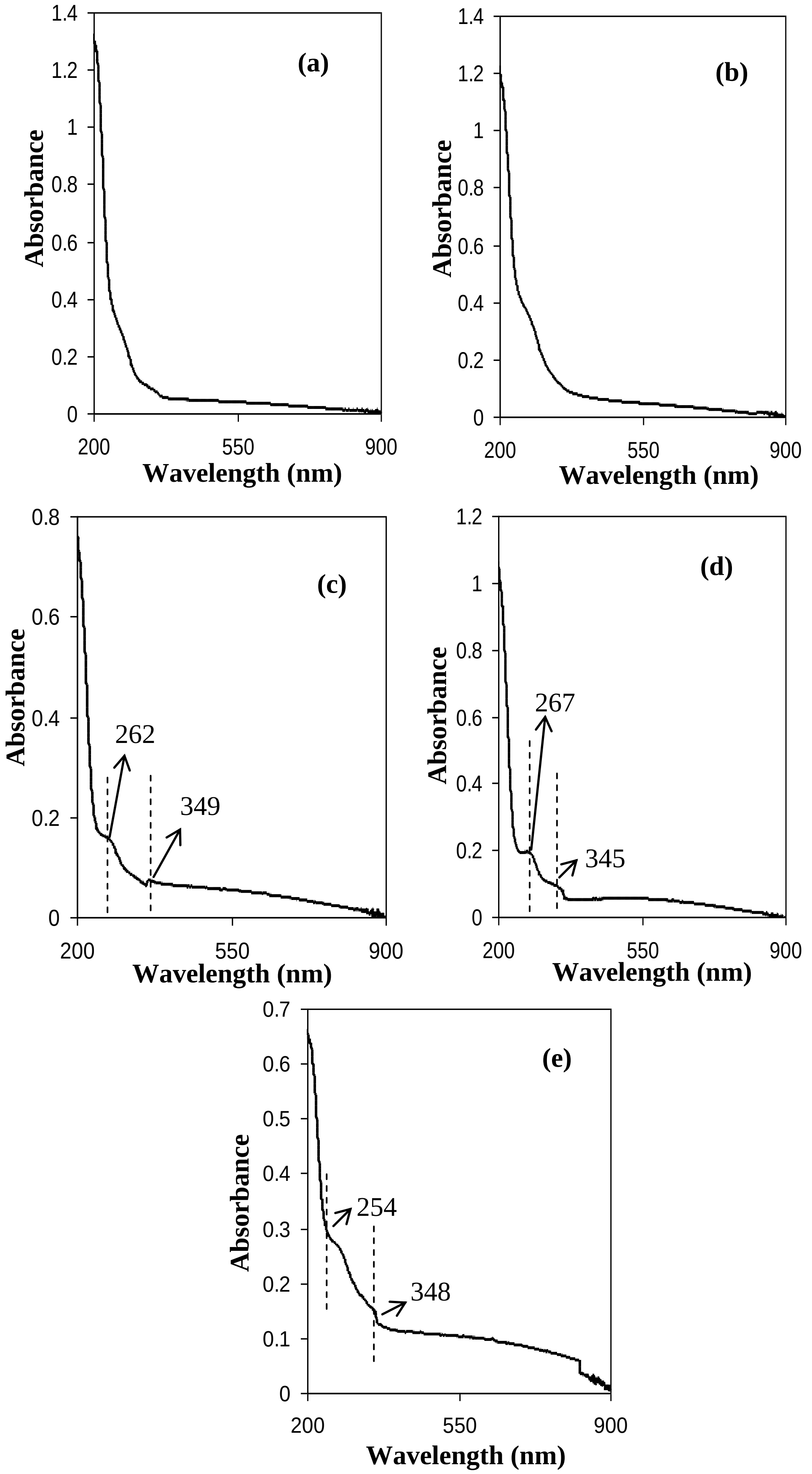

Figure 5.7: The UV-Vis absorption spectra of PVA films (dissolved in acetic acid) and doped with (a) 2 wt. %, (b) 4 wt. %, (c) 6 wt. %, (d) 8 wt. % and (e) 10 wt. % $Li_4Ti_5O_{12}$.

5.5 Scanning electron microscopy (SEM)

Figure 5.8 shows the micrographs for films of PVA dissolved in (a) water and (b) acetic acid. White spots are observed on the image of PVA film with water as solvent. White spots are also detected by Mohan *et al*., (2010) and Bhat *et al*., (2007). No white spots are found when PVA is dissolved in acetic acid solution. The surface of film is even and homogeneous because of its good film forming properties [Yang *et al*., 2009].

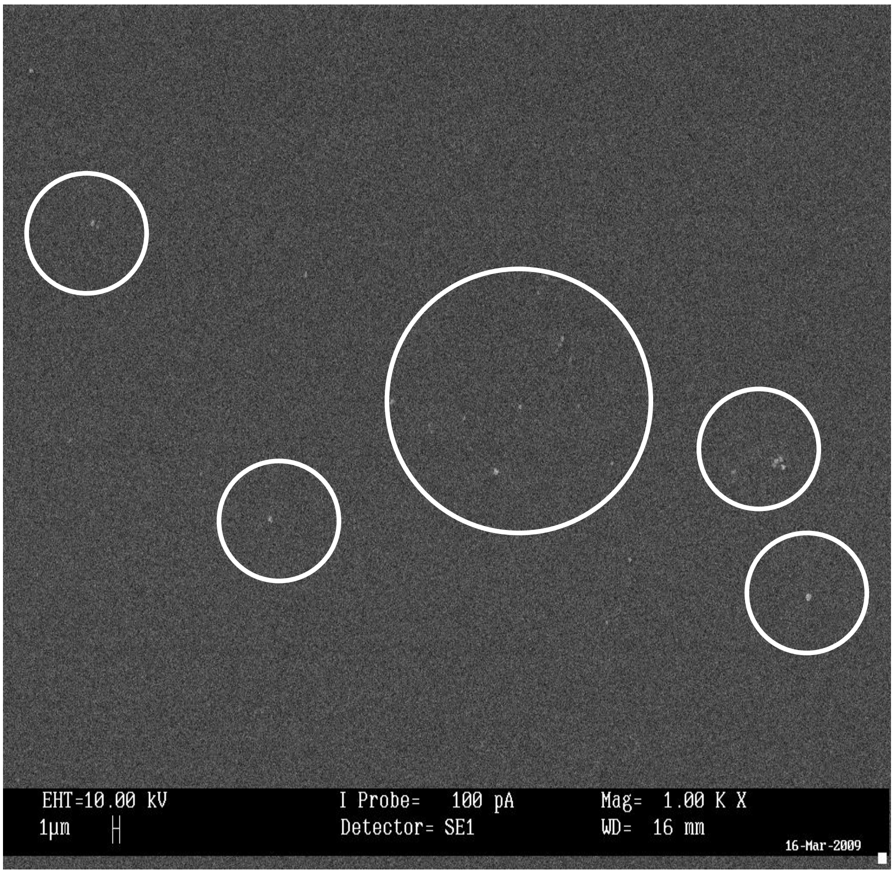

Figure 5.8 (a): SEM image of PVA film dissolved in water. Circles show some of white spots.

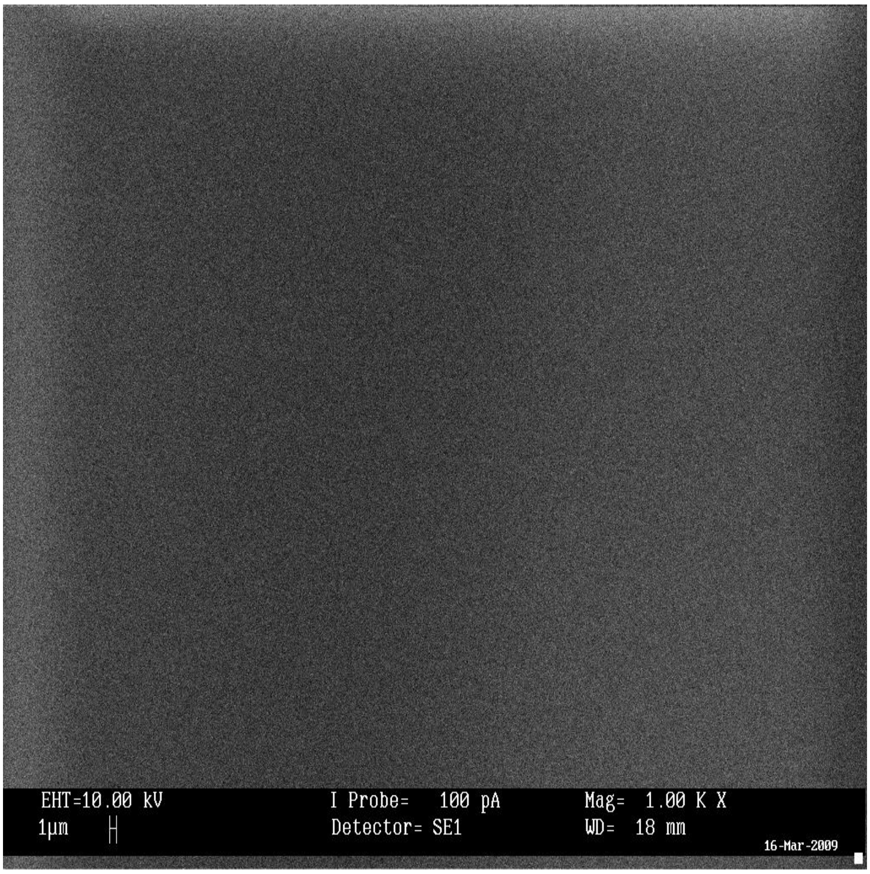

Figure 5.8(b): SEM images of PVA film dissolved in acetic acid.

Due to the even and homogeneous surface of the PVA film 1 % acetic acid as the solvent, for $Li_4Ti_5O_{12}$ doped PVA films, acetic acid will be used as the solvent. Shown in Figure 5.9 are micrographs for films of PVA dissolved in 1 % acetic acid and doped with (a) 2 wt. %, (b) 4 wt. %, (c) 6 wt. %, (d) 8 wt. % and (e) 10 wt. % $Li_4Ti_5O_{12}$. Upon addition of the oxide, the SEM micrographs show rough morphologies. Aggregates of $Li_4Ti_5O_{12}$ can be observed on the surface of the PVA film. $Li_4Ti_5O_{12}$ particles are not uniformly distributed on the surface of the films. The dispersability of the oxide particles in the polymer host is low.

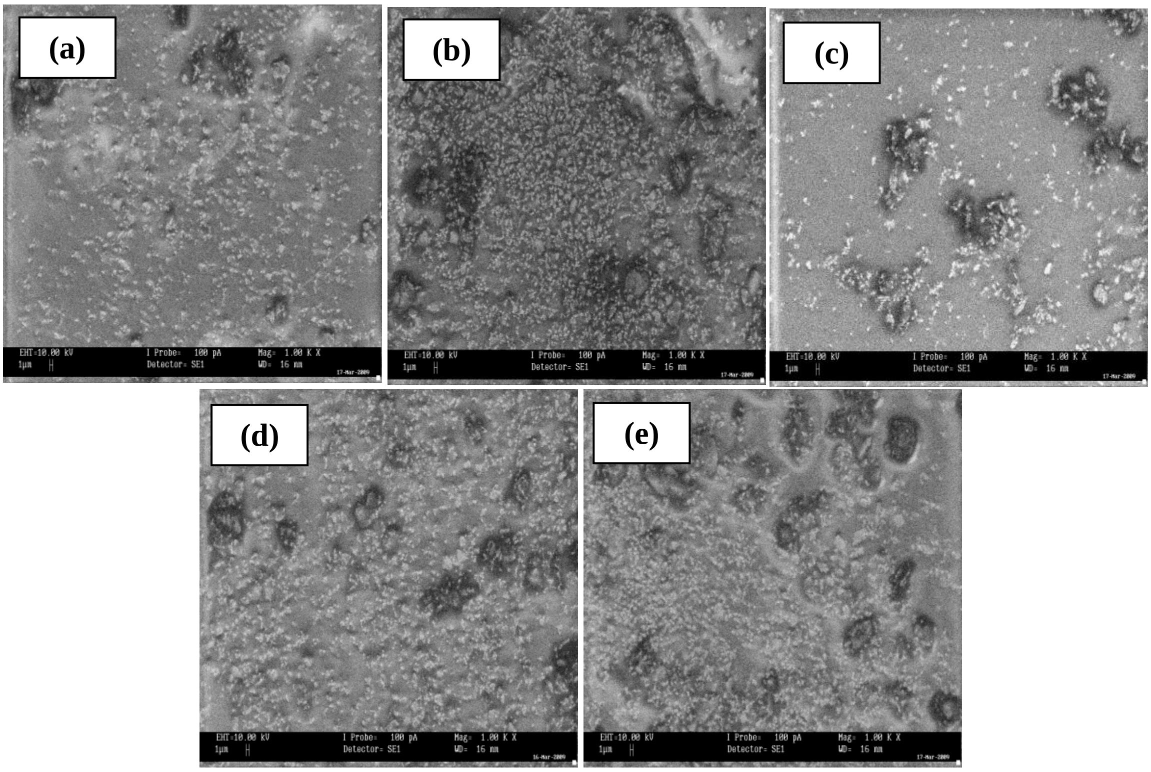

Figure 5.9: SEM images of PVA film doped with (a) 2 wt. %, (b) 4 wt. %, (c) 6 wt. %, (d) 8 wt. % and (d) 10 wt. % $Li_4Ti_5O_{12}$.

5.6 Dielectric studies

Electrochemical impedance spectroscopy (EIS) has been employed to study the effect of adding various amounts of $Li_4Ti_5O_{12}$ in the poly (vinyl alcohol) (PVA). The value of dielectric constant (ε_r), real modulus (M_r), imaginary modulus (M_i), and loss tangent (tan δ) were obtained from calculations of imaginary and real impedance data. Shown in 5.10 is the plot of ε_r versus log f for PVA films dissolved in water, 1 % acetic acid and doped with different concentrations of $Li_4Ti_5O_{12}$ at 298 K. It can be observed that dielectric constant is dependent with the frequency from 4.5 Hz to 6 Hz. As the frequency increases, the ε_r decreases.

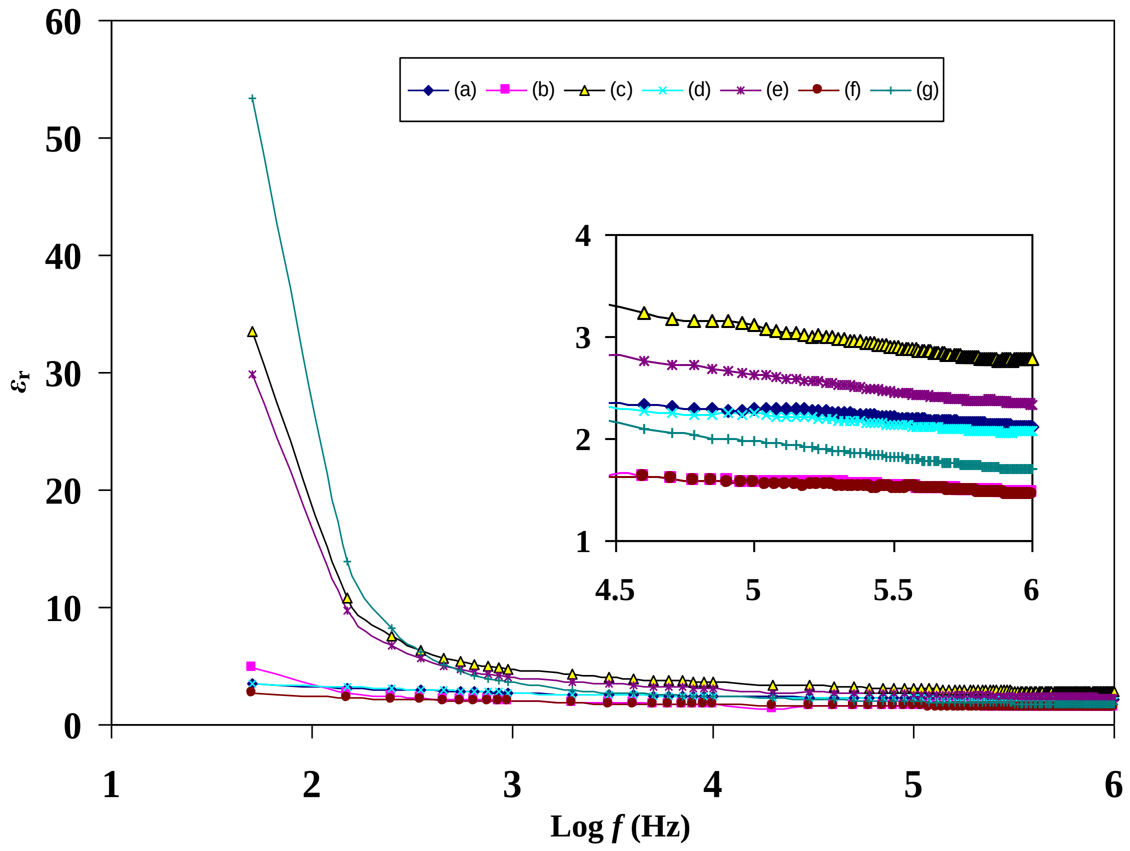

Figure 5.10: Dielectric constant (ε_r) versus log frequency of (a) PVA water, (b) PVA acetic acid, PVA doped with (c) 2 wt. %, (d) 4 wt. %, (e) 6 wt. %, (f) 8 wt. % and (g) 10 wt. % of $Li_4Ti_5O_{12}$.

Figure 5.11 shows the plot of real modulus versus log f for all films. It can be observed that as the frequency increases, M_r increases. However, no maximum peak was observed. The electric imaginary modulus response with frequency for the PVA films with different weight percentage of $Li_4Ti_5O_{12}$ is shown in Figure 5.12. No peaks were observed for films of PVA dissolved in water and for the film containing 2 wt. % of $Li_4Ti_5O_{12}$ with 1 % acetic acid as solvent. The plots of M_i versus log f for other samples show a relaxation peak.

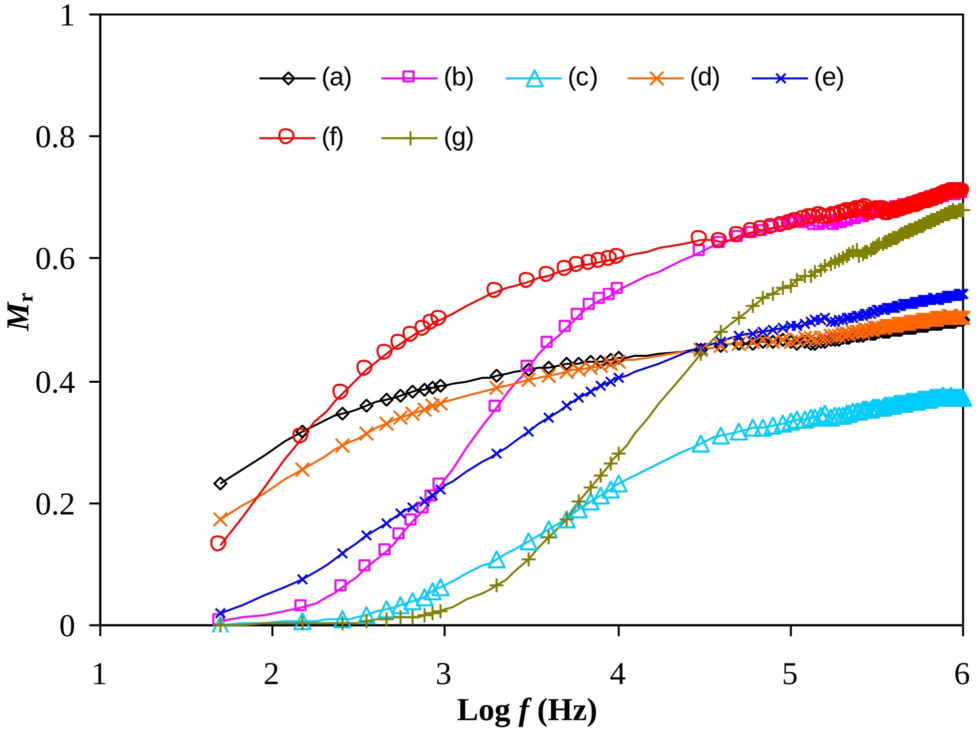

Figure 5.11: Real modulus versus log frequency of (a) PVA water, (b) PVA acetic acid, PVA doped with (c) 2 wt. %, (d) 4 wt. %, (e) 6 wt. %, (f) 8 wt. % and (g) 10 wt. % of $Li_4Ti_5O_{12}$.

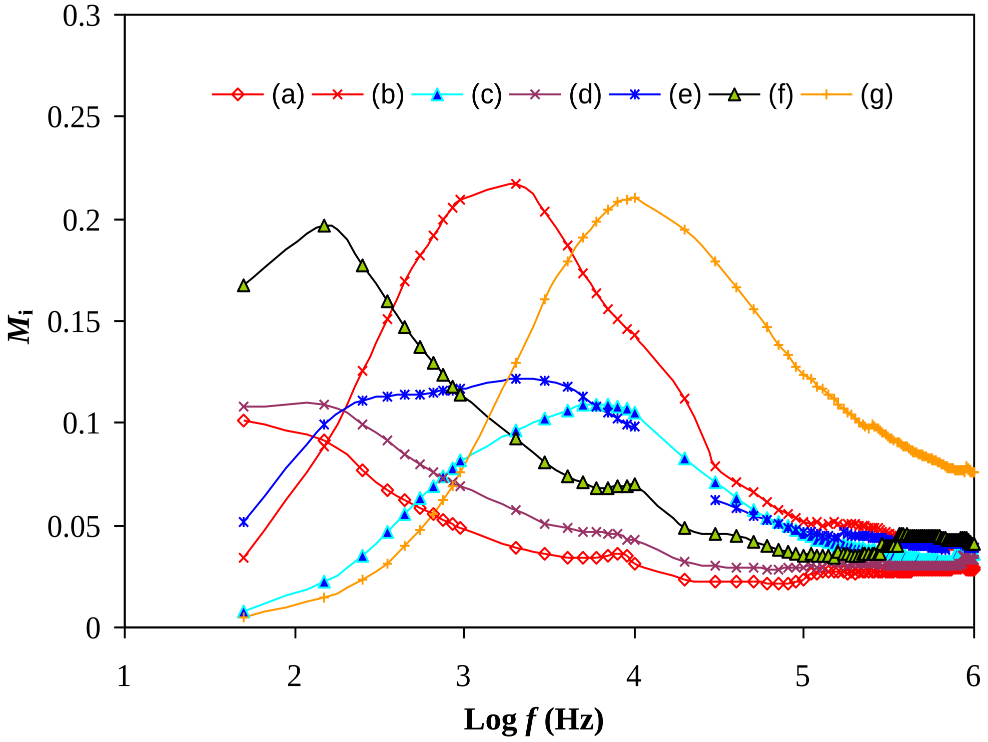

Figure 5.12: Imaginary modulus versus log frequency of (a) PVA water, (b) PVA acetic acid, PVA doped with (c) 2 wt. %, (d) 4 wt. %, (e) 6 wt. %, (f) 8 wt. % and (g) 10 wt. % of $Li_4Ti_5O_{12}$.

Mohan *et al*., (2010) noted that loss tangent or dissipation factor (tan δ) can be defined as the ratio of the loss factor to the relative permittivity and is a measurement of the ratio of the electric energy lost to the energy stored in a periodic field. Figure 5.13 shows the plot of dissipation factor versus log f for PVA film dissolved in water, acetic acid and various amounts of $Li_4Ti_5O_{12}$ at 298 K.

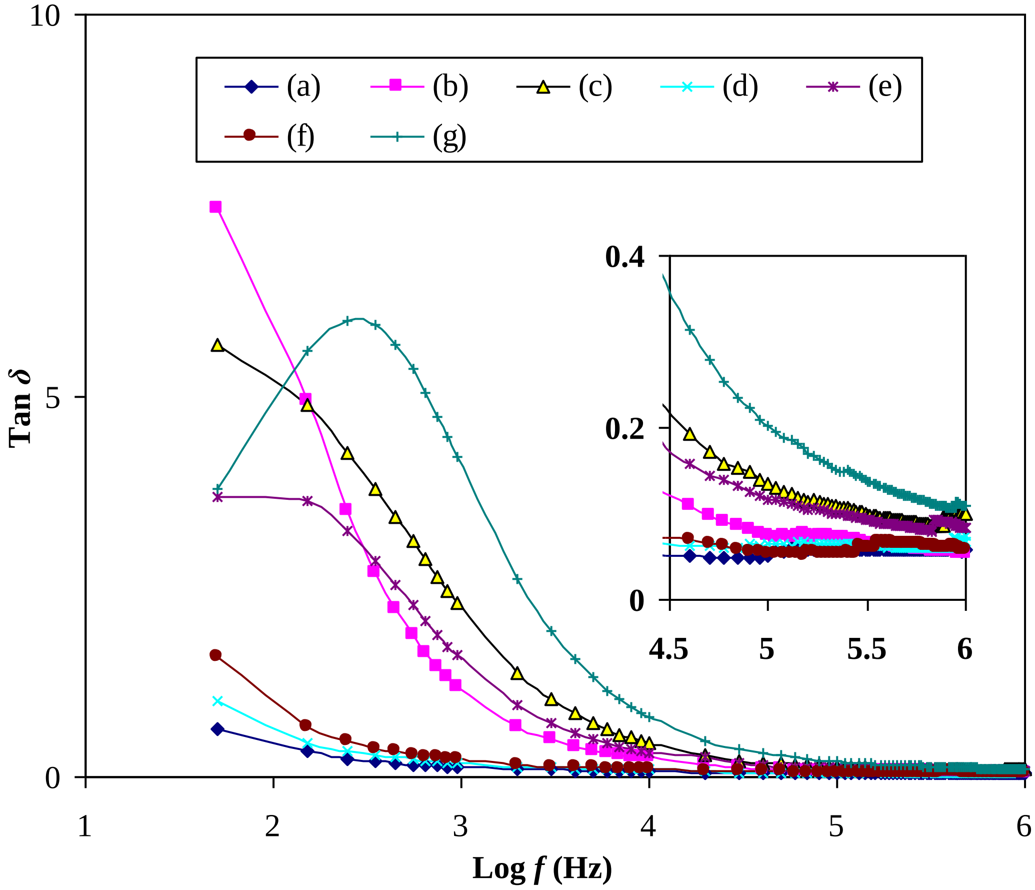

Figure 5.13: Dissipation factor (tan δ) versus log frequency of (a) PVA water, (b) PVA acetic acid, PVA doped with (c) 2 wt. %, (d) 4 wt. %, (e) 6 wt. %, (f) 8 wt. % and (g) 10 wt. % of $Li_4Ti_5O_{12}$.

Figure 5.14 shows the tan δ versus log frequency plot at various temperatures for film of PVA dissolved in water. It can be observed that no peak is exhibited for temperatures from 298 K to 333 K. Shown in Figure 5.15 is loss tangent for films of PVA dissolved in acetic acid. No peaks can be observed at temperatures 298 K, 303 K and 313 K.

However at 323 K and above, each plot exhibits a relaxation peak which is shifted to higher frequency as the temperatures increase.

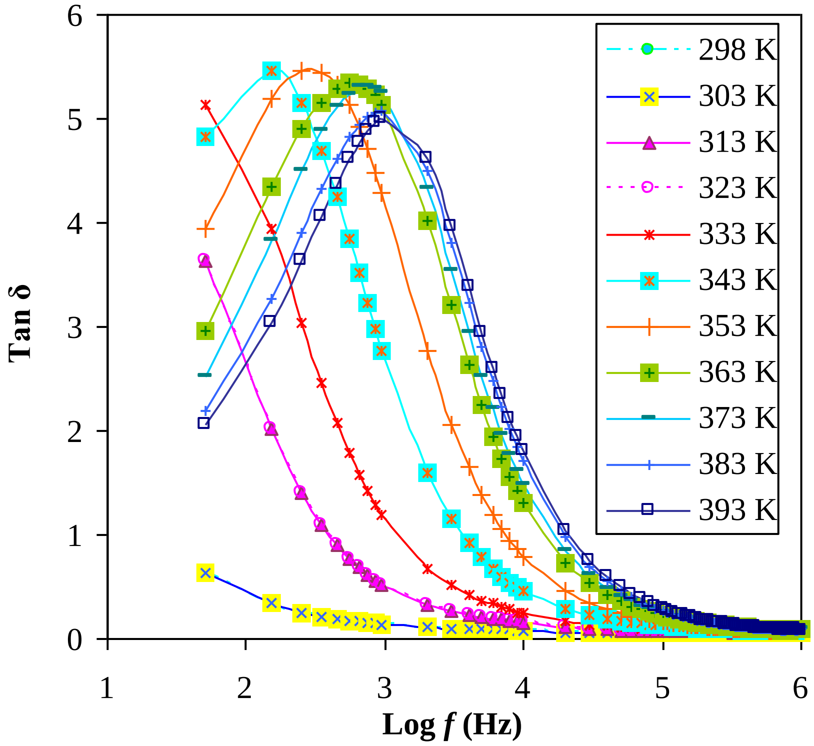

Figure 5.14: Tan *δ* versus log *f* (Hz) at various temperatures for film of PVA dissolved in water.

Shown in Figure 5.16 is the plot of tan *δ* versus log *f* (Hz) for PVA dissolved in 1 % acetic acid doped with 2 wt. % $Li_4Ti_5O_{12}$ at various temperatures. It can be observed that at temperatures 298 K and 303 K, no relaxation peaks are exhibited and from 313 K, the relaxation peaks are observed. As the temperatures increases, the peak shifts to higher frequency.

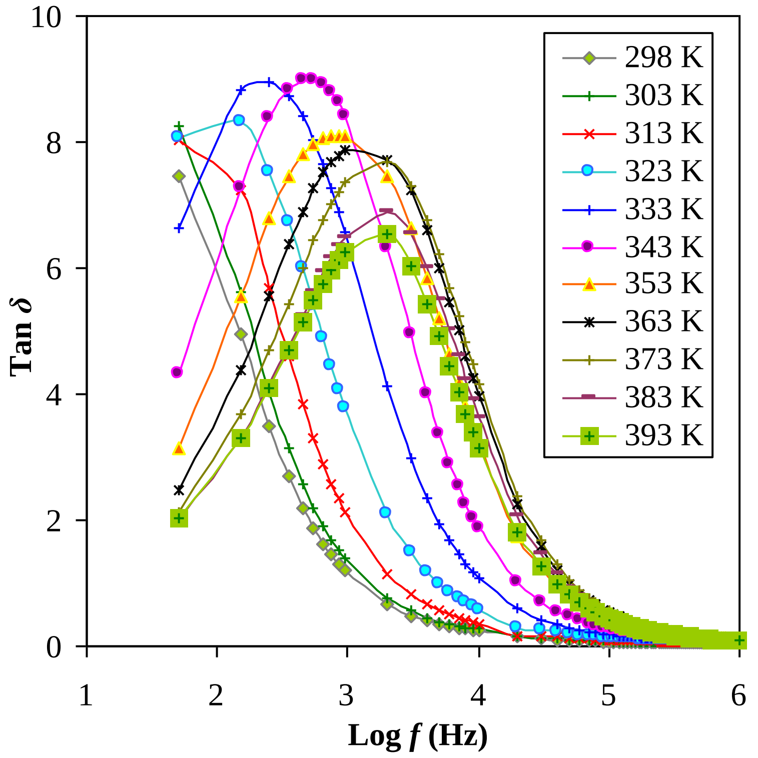

Figure 5.15: Tan δ versus log *f* (Hz) at various temperatures for film of PVA dissolved in acetic acid solvent.

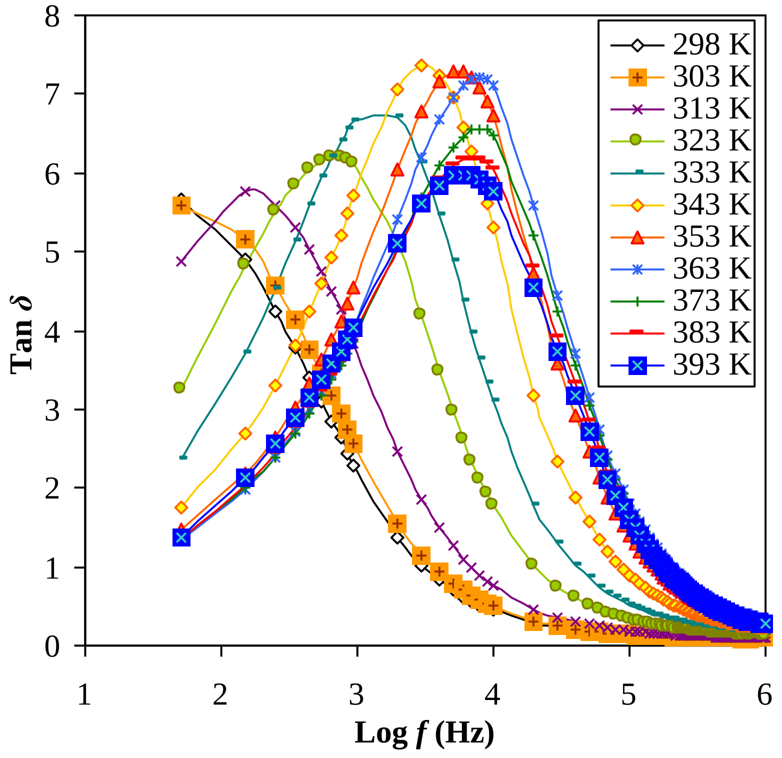

Figure 5.16: Tan δ versus log *f* (Hz) at various temperatures for films of PVA doped with 2 wt. % $Li_4Ti_5O_{12}$.

Shown in Figure 5.17 is the plot of tan δ versus log frequency at various temperatures for PVA dissolved in 1 % acetic acid and doped with 4 wt. % $Li_4Ti_5O_{12}$. Tan δ is found to increase with the frequency at different temperatures, passes through a maximum value (tan $\delta)_{max}$ and thereafter decreases. It can also be observed that as the temperature increased, the frequency at which (tan $\delta)_{max}$ occurs shifted to higher frequencies.

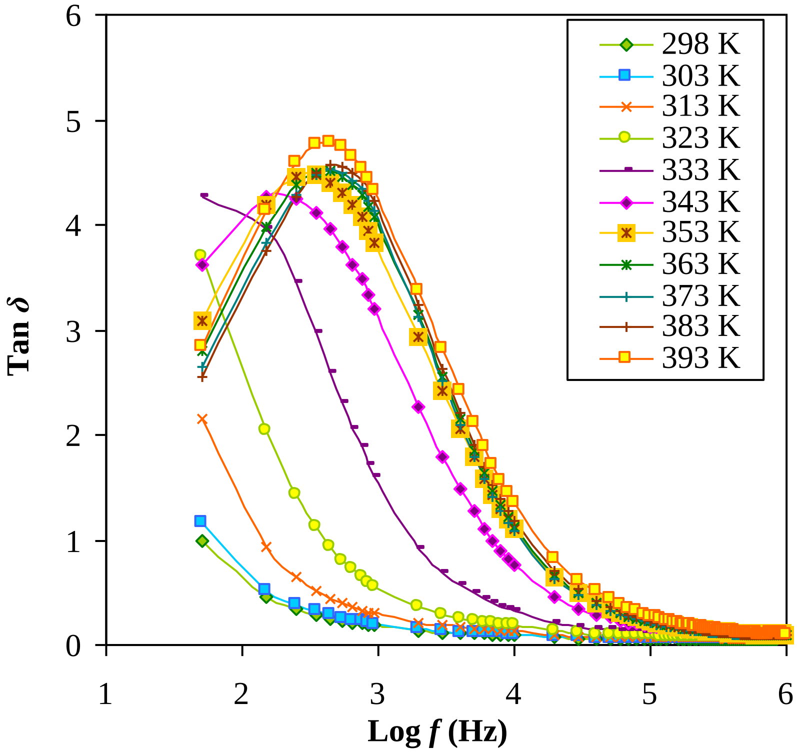

Figure 5.17: Tan δ versus log f (Hz) at various temperatures for films of PVA doped with 4 wt. % $Li_4Ti_5O_{12}$.

Shown in Figure 5.18 is loss tangent versus log frequency for film containing 6 wt. % of $Li_4Ti_5O_{12}$. It can be observed that relaxation peaks are observed at all temperatures. The height peak representing the highest temperature is the lowest compared to others and the highest relaxation peak can be seen at 343 K. Figure 5.19 is a plot of loss tangent for the film containing 8 wt. % of $Li_4Ti_5O_{12}$ at different temperatures. It can be observed that no maximum tangent loss for the first four temperatures. From 333 K to 393 K, the peak can be seen clearly. The peaks shift to high frequency as the temperature increase.

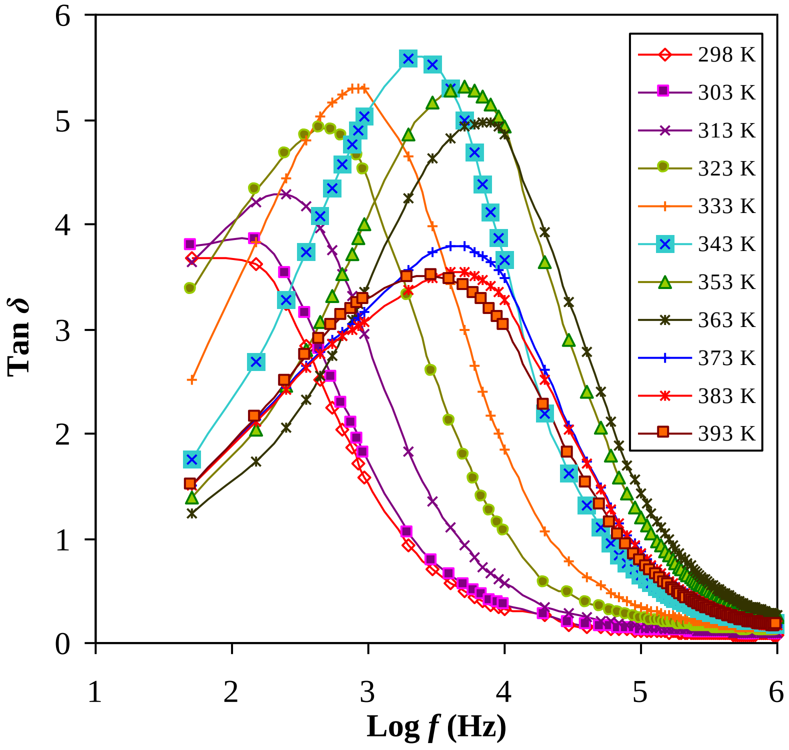

Figure 5.18: Tan *δ* versus log *f* (Hz) at various temperatures for films of PVA doped with 6 wt. % $Li_4Ti_5O_{12}$.

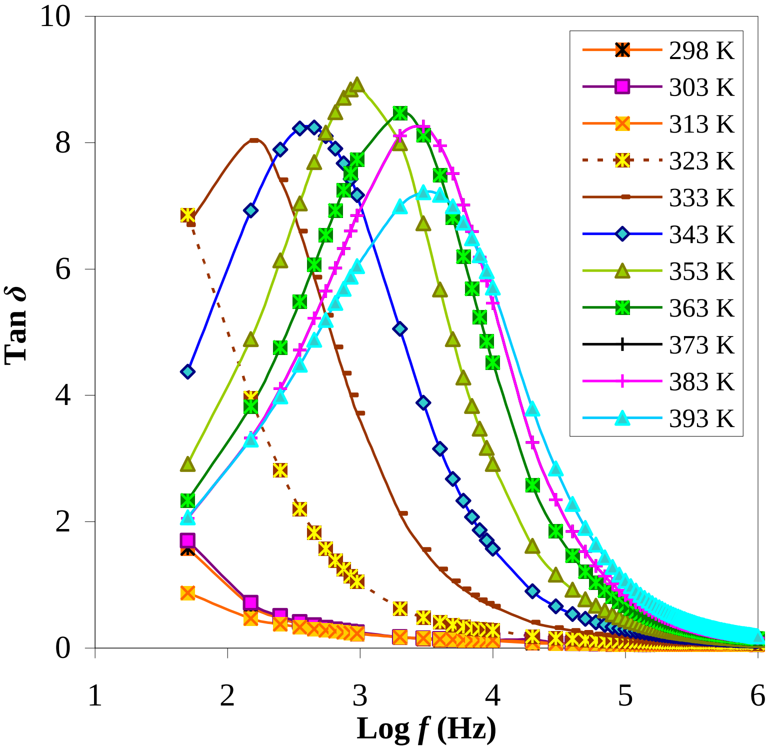

Figure 5.19: Tan *δ* versus log *f* (Hz) at various temperatures for films of PVA doped with 8 wt. % $Li_4Ti_5O_{12}$.

Figure 5.20 shows the tan *δ* against log *f* (Hz) for PVA doped with 10 wt. % of $Li_4Ti_5O_{12}$ from 298 K to 393 K. It can be observed that relaxation peaks are exhibited at all temperatures.

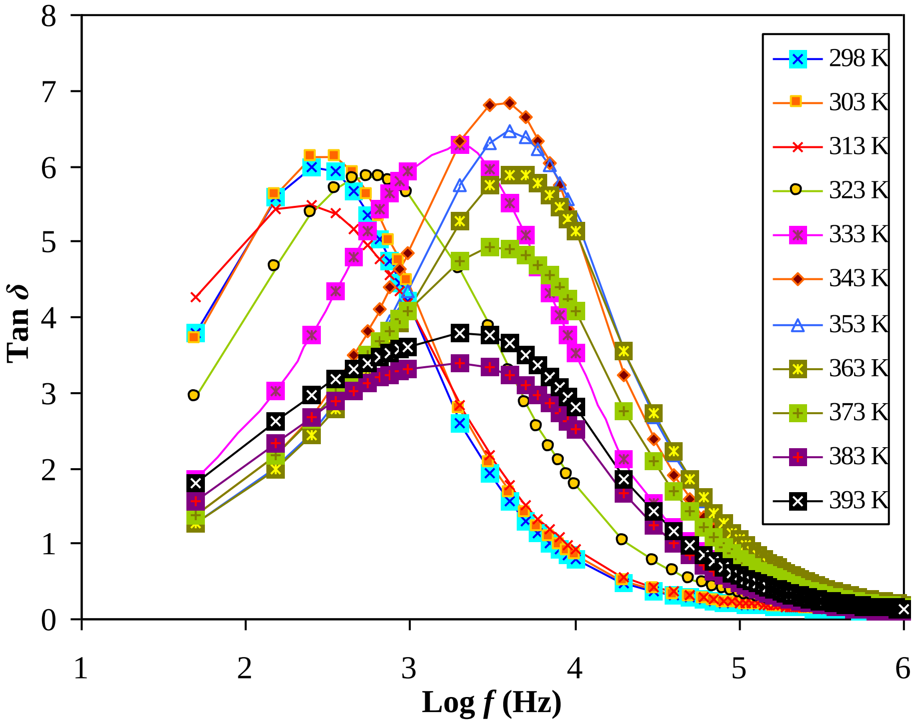

Figure 5.20: Tan *δ* versus log *f* (Hz) at various temperatures for films of PVA doped with 10 wt. % $Li_4Ti_5O_{12}$.

Since $Li_4Ti_5O_{12}$ is not uniformly distributed in the PVA film and the dissipative loss by the PVA/$Li_4Ti_5O_{12}$ composite is quite high as compared to PVDF/$BaTiO_3$ composite, it may be inferred that the composite studied in this work is not quite suitable as a dielectirc materials for capacitors.

5.7 Dielectric relaxation process

Ayesh (2008) noted that on exposure the dielectric materials to an alternating electric field, the displacement polarization leads to electrical oscillations. Due to inertia, the orientational polarization of the dipoles does not responde immediately to the change of electric field and is therefore always retarded. This process is called dielectric relaxation. Dielectric relaxation can be divided into two; conductivity and viscoelastic relaxations. Viscoelastic relaxation is due to the dipolar relaxation. Conductivity relaxation is the process due to the translational diffusion of ions which causes conduction. The conductivity relaxation corresponds to the Debye model and with only a single relaxation time. Viscoelastic relaxations are known to exhibit a distribution of relaxation times [Mohomed *et al*., 2005]. Pissis and Kyritsis (1997) noted that in the modulus formalism, the space charge effects are suppressed and an ionic conductivity peak is revealed. Plot of M_i versus M_r proceed from lower to higher frequencies [Mohomed *et al.*, 2005]. Argand plots of M_i versus M_r can be designed from the following equation.

$$\left\{M_r - \frac{(M_U + M_R)}{2}\right\}^2 + (M_i)^2 = \left(\frac{M_U + M_R}{2}\right)^2$$

where M_U and M_R represents electric modulus values at high frequency, unrelaxed state and at low frequency, relaxed state. If a perfect semicircular shape is obtained with its centre on the horizontal axis, then dielectric relaxation is conductivity relaxation. Otherwise it is viscoelastic relaxation. The Argand plots are shown in Figure 5.21 for PVA film dissolved in water and in 1 % acetic acid solvent. The Argand plots do not show prefect semicircles with centre on the x-axis. Similar trend of imprefect semicircular shape is shown in Figure 5.22 for samples of PVA doped with different amounts of $Li_4Ti_5O_{12}$ and dissolved in 1 % acetic acid solvent.

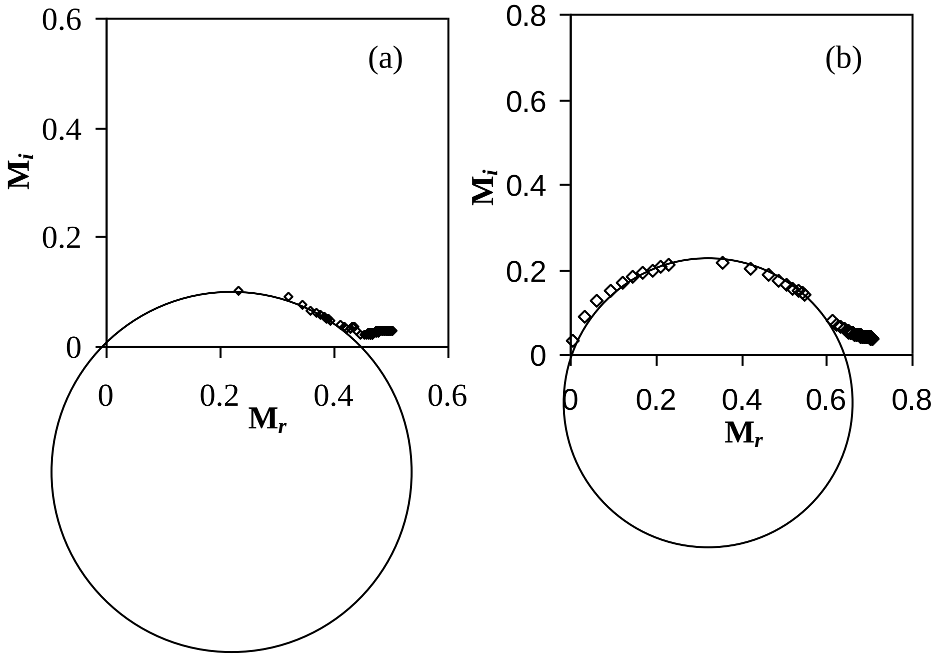

Figure 5.21: Argand plots derived from the conductivity relaxation region for pure PVA based solvent (a) water and (b) acetic acid.

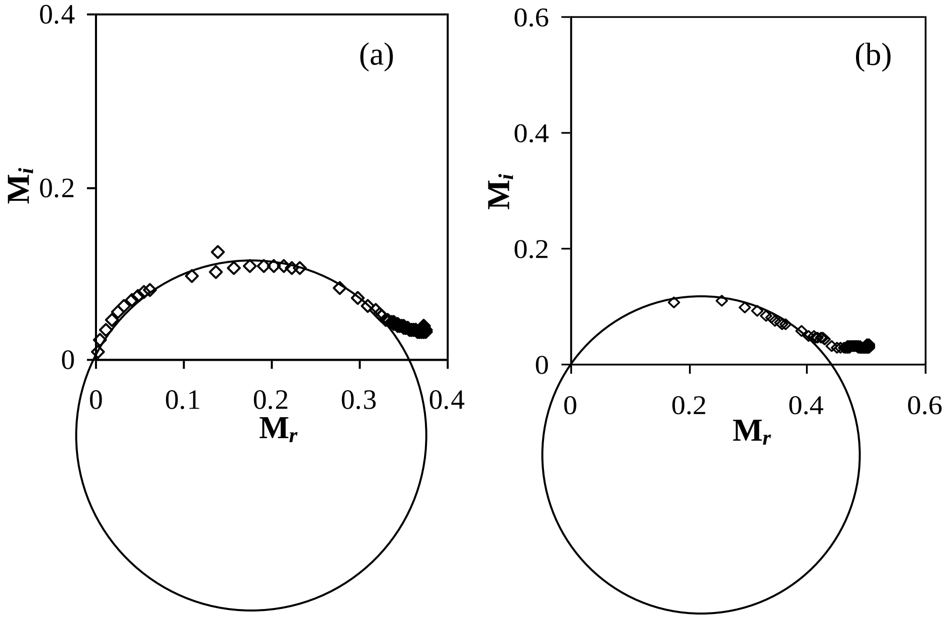

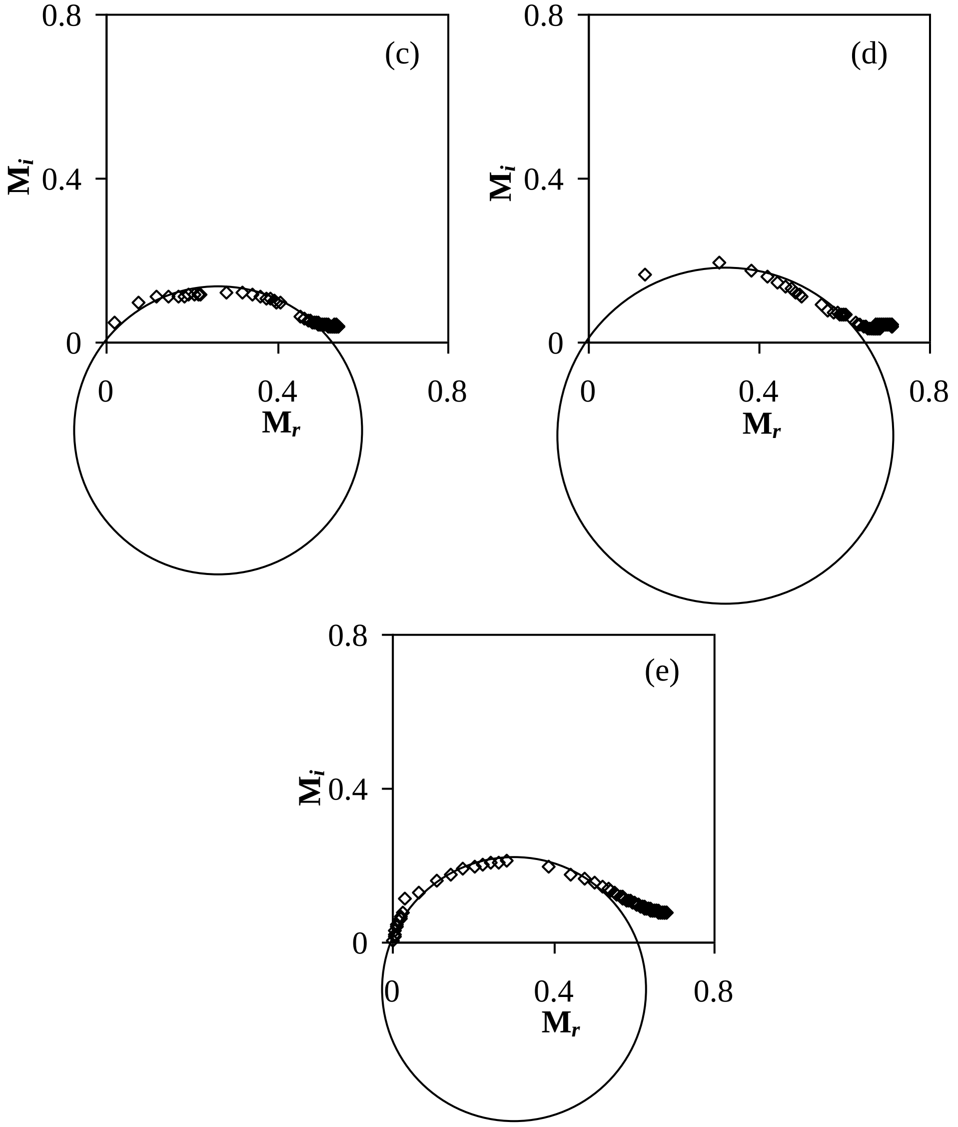

Figure 5.22: Argand plots PVA doped with different concentrations of $Li_4Ti_5O_{12}$ (a) 2 wt. %, (b) 4 wt. %, (c) 6 wt. %, (d) 8 wt. % and (e) 10 wt. %.

5.8 Summary

PVA films doped with lithium titanate are successfully obtained via solvent casting technique. As the weight percentage of lithium titanate increases, the film turns from transparent to opaque. From XRD, it can be observed that the PVA films become more crystalline on addition increasing $Li_4Ti_5O_{12}$ contents. From the FTIR spectra, C=C stretching is the suitable place for polaron/bipolaron to occur and is observed to shift from lower wavenumber (1571 cm^{-1}) to higher wavenumber (1583 cm^{-1}). UV-vis profiles show that as the amount of $Li_4Ti_5O_{12}$ increases, the absorption edge move to lower wavelength from 273 nm to 254 nm. SEM images show that after addition $Li_4Ti_5O_{12}$ into PVA polymer, the surface become rough and uneven. From loss tangent studies, it can be observed that at lower temperatures in the range between 298 K and 303 K the relaxation peak is not exhibited except for PVA doped with 10 wt. % of $Li_4Ti_5O_{12}$. The dielectric relaxation of PVA/$Li_4Ti_5O_{12}$ film from Argand plot is viscoelastic type.